

# Model-Based Reconstruction for Joint Estimation of $T_1$ , $T_2^*$ and $B_0$ Inhomogeneity Maps Using Single-Shot Inversion-Recovery Multi-Echo Radial FLASH

Xiaoqing Wang<sup>1,2</sup>, Zhengguo Tan<sup>3</sup>, Nick Scholand<sup>4,6</sup>, Berkin Bilgic<sup>1,2</sup> and Martin Uecker<sup>4,5,6</sup>

<sup>1</sup>Athinoula A. Martinos Center for Biomedical Imaging, Massachusetts General Hospital, Charlestown, Massachusetts, USA. <sup>2</sup>Department of Radiology, Harvard Medical School, Boston, Massachusetts, USA. <sup>3</sup>Department of Artificial Intelligence in Biomedical Engineering, University of Erlangen-Nuremberg, Germany <sup>4</sup>Institute of Biomedical Imaging, Graz University of Technology, Austria. <sup>5</sup>Department of Interventional and Diagnostic Radiology, University Medical Center Göttingen, Germany <sup>6</sup>German Centre for Cardiovascular Research (DZHK), Partner site Göttingen, Germany.

## Introduction

Inversion-recovery (IR) Look-Locker and multi-echo gradient-echo are two commonly-used sequences for  $T_1$  mapping, and water-fat,  $T_2^*$  imaging, respectively [1-6]. Recently, these two sequences have been combined in one single scan for simultaneous multi-parameter mapping [6-9], providing complementary quantitative information for clinical studies. To obtain robust parameter estimation, most existing approaches usually consist of several steps, e.g.,  $B_0$  calibration/estimation, linear image reconstruction, and pixel-wise fitting. As each step utilizes a subset of acquired data, existing approaches may have not made the best use of all available data.

In this work, we propose to jointly estimate  $T_1$ ,  $T_2^*$  and  $B_0$  maps directly from the k-space data acquired from a single-shot IR radial multi-echo FLASH by formulating parameter estimation as a nonlinear inverse problem [10-11]. In this way, all acquired data can be exploited for a joint reconstruction. Furthermore, prior knowledge such as joint sparsity and  $B_0$  smoothness can be applied directly to parameter maps to improve the conditioning of the inverse problem.

## Methods

### Sequence Design and Model-based Reconstruction

The IR multi-echo sequence is shown in Fig.1. It starts with a non-selective inversion pulse, followed by a continuous radial multi-echo spoiled gradient-echo (FLASH) using the small golden-angle readout. The signal evolution for this process can be described as:

$$S_{T_{1n}, TE_m} = \left[ W_{ss} - (W_{ss} + W_0) \cdot \exp(-T_{1n} \cdot R_{1,W}^*) \right. \\ \left. + (F_{ss} - (F_{ss} + F_0) \cdot \exp(-T_{1n} \cdot R_{1,F}^*)) \cdot z_m \right] \\ \cdot \exp(TE_m \cdot i2\pi f_{B_0}) \cdot \exp(-TE_m \cdot R_2^*). \quad (1)$$

Where  $(W_{ss}, W_0, R_{1,W}^*)^T$  are the steady-state signal, the equilibrium-state signal and the effective  $T_1$  relaxation rate for water and  $(F_{ss}, F_0, R_{1,F}^*)^T$  represent the corresponding signal components for fat.  $z_m$  is the 6-peak fat spectrum,  $f_{B_0}$  represents the field inhomogeneity and  $R_2^*$  is the  $T_2^*$  relaxation rate.  $T_{1n}$  and  $TE_m$  denote the  $n$ -th inversion time and  $m$ -th echo time, respectively. The unknowns optimized for are  $\mathbf{x} = (W_{ss}, W_0, R_{1,W}^*, F_{ss}, F_0, R_{1,F}^*, f_{B_0}, R_2^*)^T$ . Their estimation is formulated as a nonlinear inverse problem:

$$\mathbf{x} = \operatorname{argmin}_{\mathbf{x} \in D} \sum_{T_1} \sum_{TE} \|PFC \cdot S_{T_{1n}, TE_m}(\mathbf{x}) - Y_{T_{1n}, TE_m}\|_2^2 + R(\mathbf{x}). \quad (2)$$

Here  $D$  is a convex set, ensuring non-negativity of all relaxation rates and  $R(\mathbf{x})$  is a regularization term. We adopt a joint l1-Wavelet sparsity constraints [11] on all parameters of  $\mathbf{x}$  except  $f_{B_0}$ . The latter is regularized with a smoothness enforcing Sobolev penalty [12] also added to the coil sensitivities. The nonlinear inverse problem in Eq.2 is solved with a IRGNM-FISTA [11] using BART [13].

## Experiments

All MRI studies were conducted on a 3T scanner (Magnetom Skyra, Siemens Healthineers, Erlangen, Germany) with approval of the local ethics committee. The brain study was conducted using a 20-channel head/neck coil. The acquisition parameters were: FOV=192 × 192 mm<sup>2</sup>, matrix size=256 × 256, slice thickness = 5 mm, 7 echos with TR=15.6 ms TE<sub>1-7</sub>=2.36/4.26/6.16/8.06/9.96/11.90/13.80 ms, FA=6°, bandwidth=810 Hz/pixel and 450 excitations in total with 3350 radial acquired spokes. Nice spokes were combined into one  $k$ -space frame for fast computation.

## Results & Discussion

The proposed model-based reconstruction was first validated for a numerical phantom, which provides ground truth in the presence of noise. Fig.2(A) presents the determined quantitative water  $T_1$ , fat  $T_1$ ,  $T_2^*$  and  $f_{B_0}$  maps from the model-based reconstruction. Fig.2(B) shows the corresponding Bland-Altman plots comparing quantitative values estimated from ROIs to the known ground truth. The small differences observed in the Bland-Altman plots confirm good accuracy for all parameter maps.

Fig.3 further demonstrates model-based reconstructed brain water  $T_1$ , fat  $T_1$ ,  $T_2^*$  and  $f_{B_0}$  maps. The steady-state water and fat images (i.e.,  $W_{ss}$  and  $F_{ss}$  in Eq.1) are additionally shown in the second row. Although a reference method need to be performed for a pairwise comparison, visual inspection shows artifact-free quantitative  $T_1$  and  $T_2^*$  maps. The quantitative values estimated from ROIs ( $T_1$ : white matter: 800±8 ms gray matter: 1388±61 ms;  $T_2^*$ : white matter: 46±2 ms gray matter: 61±3 ms) correspond well to the literature values [4,10].

## Summary

The presented work formulates the joint estimation of  $T_1$ ,  $T_2^*$  and  $f_{B_0}$  maps from a single-shot IR multi-echo acquisition as a single nonlinear inverse problem. Initial results on a simulated phantom and a healthy subject demonstrate that high resolution and artifact-free quantitative maps can be reconstructed simultaneously with the proposed method.

## References

- [1] Look DC *et al.* Rev Sci Instrum 1970;41:250-251. [2] Bernstein M *et al.* Handbook of MRI Pulse Sequences. [3] Hernando D *et al.* Magn Reson Med. 2012; 68: 830?840. [4] Tan Z *et al.* arXiv:2020.02788. [5] Schneider M *et al.* Magn. Reson. Med. 2020; 84:2592-2605. [6] Feng L *et al.* Magn. Reson. Med. 2021; 86:97-114. [7] Cao T *et al.* Magn. Reson. Med. 2022; 87:1375-1389. [8] Jaubert O *et al.* Magn. Reson. Med. 2020; 84:2625-2635. [9] Lima da Cruz GJ, *et al.* Magn. Reson. Med. 2022;87:2757-2774. [10] Block T *et al.* IEEE Trans Med Imaging 2009;28:1759-1769. [11] Wang X *et al.* Magn Reson Med. 2018;79:730-740. [12] Uecker M *et al.* Magn Reson Med 2008;60:674-682. [13] Blumenthal M *et al.* mrirecon/bart: version 0.8.00. 2022.

This work was partially funded by NIH under grant U24EB029240. We thank Dr. Li Feng for insightful discussions.

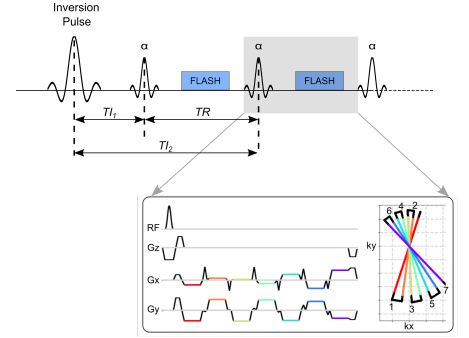


Figure 1: Schematic diagram of the inversion-recovery multi-echo FLASH sequence and its asymmetric radial sampling pattern.

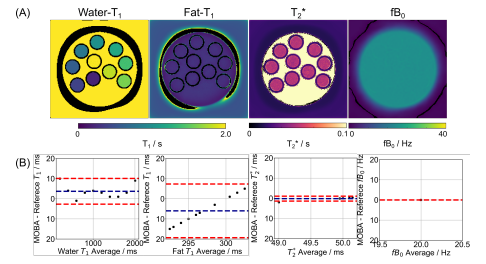


Figure 2: (A) Model-based reconstructed quantitative water- $T_1$ , fat- $T_1$ ,  $T_2^*$  and  $f_{B_0}$  maps from a single-shot IR multi-echo radial FLASH acquisition for a simulated phantom. (B) Bland-Altman plots comparing ROI-analyzed mean quantitative values to the ground truth.

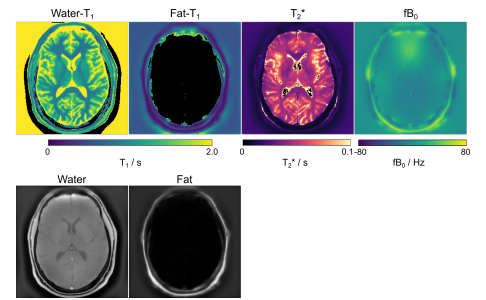


Figure 3: (Top). Model-based reconstructed artifact-free brain water  $T_1$ , fat  $T_1$ ,  $T_2^*$  and  $f_{B_0}$  maps from a single-shot IR multi-echo radial FLASH acquisition. (Bottom). Steady-state water and fat images (i.e.,  $W_{ss}$  and  $F_{ss}$  in Eq.1) from the model-based reconstruction.